Nonlinear Simulation of Wave Resonances in a Narrow Gap between Two Barges

by Xingya Feng, Wei Bai[*] and Kok Keng Ang
Department of Civil and Environmental Engineering, National University of Singapore, Singapore
E-mail: *w.bai@nus.edu.sg*

Highlights:

- Within the frame of fully nonlinear potential wave theory, the fluid field is reformulated as contributions from a prescribed nonlinear incoming wave and a scattered wave, and this separation improves computational efficiency.
- Wave resonances in the gap between two side-by-side barges are observed, and wave nonlinearity is found to contribute to the discrepancy between linear theory and experimental data near the piston-mode frequency.

1. Introduction

In the last decade, increasing examples of side-by-side operations have been seen in the marine industry when larger consumption of oil and gas is demanded. These operations could be, for instance, cargo loading and offloading from a LNG-Carrier to a FPSO or FSRU in close proximity. The resonant phenomenon of the waves trapped in the gap between two side-by-side hulls has caught great attentions. Molin [1] derived an approximation formula for estimation of the resonant frequencies from a simplified geometry, which is similar to the moonpool resonances. The resonances generate different mode shapes within the gap at each mode frequency. At the first resonant mode, i.e. the piston mode, very large free surface elevations near the midship are observed both theoretically and experimentally. However, linear software packages are reported to potentially over-predict the wave responses, namely RAOs (Response Amplitude Operators) of the free surface elevations in the gap at the piston mode. Consequently the mean drift forces on the hulls and ship motions could vary much from the predictions.

It is widely accepted that the discrepancy between the linear predictions and experimental data is mainly due to flow viscosity, i.e. vortex shedding and flow separation behind the body. Much effort has been made to tackle the abovementioned problem, through an appropriate introduction of viscous damping into the models. Newman [2] modeled a damping lid on the gap surface and used the generalized mode technique to compute the lid motions. Chen [3] introduced a damping force term into the free surface boundary conditions, which was explained as energy dissipation. However, Pauw *et al*. [4] showed that there is no *a priori* to determine the damping coefficient unless calibrated by experimental tests.

Besides that, within the frame of potential wave theory the nonlinearity associated with the free surface boundary conditions can also contribute to the discrepancy between the linear predictions and experimental data, and this aspect is not well understood at the present point of time. Recently, Kristiansen and Faltinsen [5] applied a vortex tracking method to study the piston mode in a vertical gap and concluded that flow separation mainly accounted for the discrepancy between linear results and measurements, and nonlinear free surface conditions are of minor importance. However, it should be noted that the propagating waves in their model tests are of low wave steepness, kA approximately from 0.3% to 1.0%. Therefore, wave nonlinearity is not strong when wave steepness is very low. Molin *et al*. [6] experimentally and numerically investigated the gap resonances between two rectangular barges and also concluded that the discrepancy is mostly due to the flow separation at the barge bilges, based on their experiments.

In the present study, in order to assess the importance of wave nonlinearity the same two barges as in Molin *et al*. [6] are simulated at the wave steepness kA ranging from 0.34% to some 7.8%. A fully nonlinear potential wave theory has been employed and the free surface boundary conditions are reformulated by separating the wave field into an incoming nonlinear wave and a scattered wave. With low wave steepness, free surface RAOs in the gap are generally convergent to the linear results in Molin *et al*. [6]. Interestingly, by comparing with linear results and tests, our fully nonlinear results show that the contribution of nonlinearity associated with the free surface conditions will be becoming more significant with the increase of wave steepness, which is not same as described in [5] and [6].

2. Mathematical Formulation

A circular numerical wave tank (NWT) is defined to investigate the wave-body interaction problem. Fig. 1(a) presents the bird view of employed NWT model, including a circular tank, two rectangular barges, free water surface and a damping zone near the tank side wall. The origin of a coordinate system $Oxyz$ is placed at the center of the gap on the calm water surface, with z-axis pointing upwards. Direction of incident wave is denoted by β, and the damping zone has a width of one wave length.
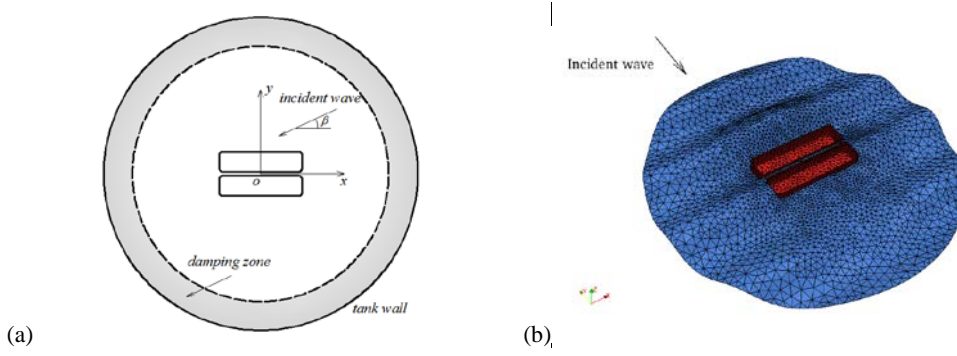
Fig. 1 NWT model with two side-by-side barges: (a) sketch of bird view, (b) 3D mesh

It is practical and computationally economical to separate the total flow into an incident flow and a scattered field. This actually has been applied in the linear theory. When we rewrite the total velocity potential as $\phi = \phi_I + \phi_S$ and the position of water particles on the free water surface as $\mathbf{X} = \mathbf{X}_I + \mathbf{X}_S$, the governing Laplace equation remains linear and the scattered potential ϕ_S satisfies

$$\nabla^2 \phi_S = 0 \tag{1}$$

Substituting the total potential and position into the corresponding boundary conditions leads to the following new conditions on the free surface and the rigid boundary for the scattered wave,

$$\frac{\mathrm{D}\mathbf{X}_S}{\mathrm{D}t} = \nabla\phi - \nabla\phi_I \tag{2}$$

$$\frac{\mathrm{D}\phi_S}{\mathrm{D}t} = -gz_S + \frac{1}{2}\nabla\phi\cdot\nabla\phi - \frac{1}{2}\nabla\phi_I\cdot\nabla\phi_I \tag{3}$$

$$\frac{\partial\phi_S}{\partial n} = -\frac{\partial\phi_I}{\partial n} \tag{4}$$

where D/Dt stands for the material derivative, g is the gravitational acceleration, and the subscripts 'I' and 'S' denote the quantities for incident and scattered waves respectively. The potential, velocity and positions due to the incident waves are all specified explicitly. In the damping zone, only the scattered wave near the tank wall will be damped.

Here, the incoming flow is prescribed as a regular 5th order Stokes wave. Further information on the higher order boundary element simulation in time domain can be found in Bai and Eatock Taylor [7].

3. Comparisons with Linear Theory and Experiments

We consider the case of two fixed barges described in Molin *et al.* [6]. The barges are of length 2.47 m, width 0.6 m and draft 0.18 m, and they are separated by a gap of width 0.12 m. The water depth is 3 m and tank radius is chosen 4 times the incident wave length or 2.5 times the barge length, whichever is larger. Here we focus on the cases of 90° heading, where the resonances are more interesting. Fig. 1(b) shows an example of mesh for a case of 90° incoming waves.

In order to compare our numerical results with those from linear theory, we firstly utilize a relatively low wave steepness kA of about 0.34%, where the amplitude A is defined as half the wave height of the incident wave. It is expected that our results should be close to the linear results in this case and nonlinear effect is not prominent. Fig. 2 shows the comparisons of free surface RAOs (maximum wave elevation at two different stations non-dimensionalised by A) between present results, experimental data and linear results in Molin *et al.* [6]. In their paper, the linear results were produced by the linear software DIODORE and the experimental data was extracted through a spectral analysis of the measured elevations, when the system is subjected to an irregular wave with the Pierson-Moskowitz spectra of a significant wave height $H_s = 0.02$ m and a peak period $T_p = 1.0$ s. It is found that the present free surface RAOs with low wave steepness agree quite well with the linear results both at station (0.0, 0.0) and (0.6, 0.0), though there exists difference with the experiments near the resonant frequencies. This will be discussed in the next section.

The three peaks appearing in the gap free surface RAOs are of our interest. The corresponding frequencies are near 5.75 rad/s, 6.85 rad/s and 8.0 rad/s, which are called mode frequencies. To illustrate the mode shapes near these three frequencies, we plot the free surface elevations along the narrow gap in Fig. 3. Note that the elevations are symmetric about the midship. The first mode or piston mode generates a maximum elevation over 6 times the incident wave amplitude near midship and the wave elevation decays from midship to the barge ends. The second mode or longitudinal sloshing mode shows three peaks in the gap, which are located at $x = 0.0$ m, $x = \pm 0.85$ m, and the similar resonant phenomenon appears in the third mode.
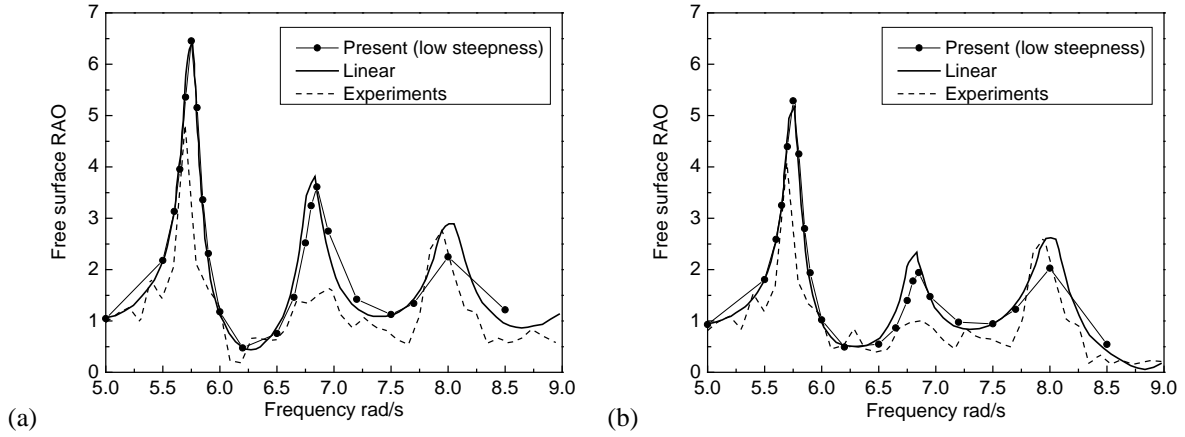
Fig. 2 Comparisons of gap free surface RAOs with linear results and experiments at: (a) $x = 0.0$ m; (b) $x = 0.6$ m, with 90° heading wave
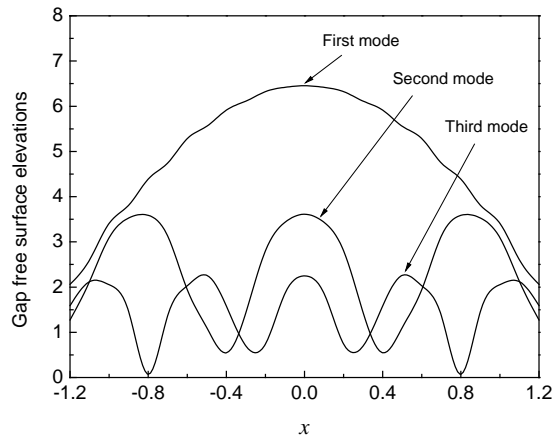

Fig. 3 Resonant mode shapes along the narrow gap between two barges with 90° heading wave

4. Nonlinear Effects

The key issue that we are trying to throw light on is the nonlinear effect of the free surface boundary conditions. We focus on the piston mode which is more critical than others. Linear theory is typically reported to over-predict the response near resonance due to lack of damping. In real flow, the existence of damping limits the amplification of free surface elevation near piston mode. We believe two mechanisms could act as system damping. The first one is the flow viscosity which may generate vortex shedding and flow separation at the barge corners. This is not modelled in the framework of potential theory. The second is the nonlinear effects associated with the free surface conditions.

To illustrate this nonlinearity, we compute the free surface RAOs at midship at the piston-mode frequency $\omega = 5.75$ rad/s for various wave steepness kA. The responses are plotted in Fig. 4. The horizontal solid line represents the linear result in Molin *et al*. [6], which is independent with wave steepness. The two dash lines are reference values of peak elevations from Molin's experimental data. The case of low significant wave height $H_S = 0.02$ m stands for mild sea state, while the large one $H_S = 0.06$ m for rough sea state. If we take half of the significant wave height as amplitude A and calculate wave number k from peak wave length, these two sea states correspond to $kA = 0.0402$ and $kA = 0.121$. Our fully nonlinear results are processed by FFT and linear and higher order harmonic components are decomposed. Fig.4 includes both the first and second harmonic components. The total maximum elevations are not presented because they are close to the first harmonic components, though second harmonics are visible in Fig. 4. The reason is that the first and second harmonics are not in phase of each other. At $kA = 0.0402$, the present result is closer to the experiment than the linear one, yet there is still some discrepancy from the experiment, which is due to the viscous effect. The viscosity must exist in the real flow, but the fully nonlinear potential wave model cannot account for it. Nevertheless, in a global view, our fully nonlinear results are increasingly approaching to the experiments with the growth of wave steepness kA. This may suggest that the contribution of the wave nonlinearity could become significant when wave steepness is high and must be considered as an important role. On the other hand, when the wave is very mild, the fluid viscosity seems to be predominant over the wave nonlinearity. In such case, the potential wave model cannot avoid over-predicting the wave elevation, even though the absolute dimensional value of this discrepancy may be relatively

small due to the small incident wave amplitude. Furthermore, another interesting phenomenon is that the first harmonics in the fully nonlinear simulation is not independent with the wave steepness, which is quite different to the linear solution. The reason is that in the fully nonlinear simulations Taylor series expansion is not adopted and the computational mesh is distributed on the actual domain boundary surface at every time step. Therefore, at higher wave steepness the fully nonlinear simulation, in principle, remains accurate, while the first order solution is questionable because the Taylor series expansion might not validate at such high wave steepness. In view of this, the generation of mesh on the real domain surface, rather than on the mean position, can have a remarkable influence on the results.
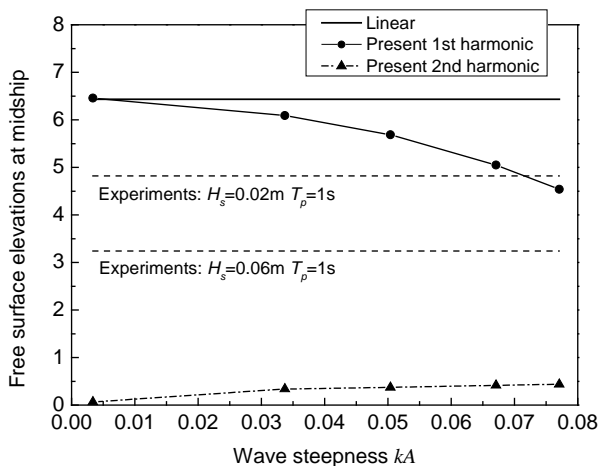

Fig. 4 Midship free surface RAOs under different wave steepness at piston-mode frequency ω = 5.75 rad/s
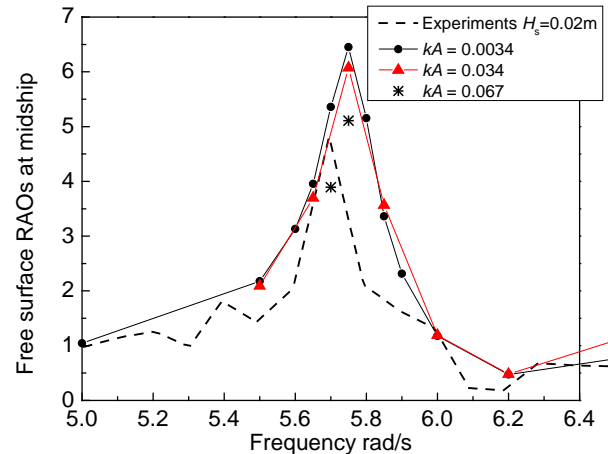
Fig. 5 Free surface RAOs at midship under different wave steepness

Fig. 5 shows more results for three different wave steepness at several frequencies. It is noticed that there is small frequency shift from the experiments at the piston mode. The reason is currently not clear, and it should be mentioned that similar phenomenon has also been observed in the study of Kristiansen and Faltinsen [5]. The free surface RAOs at midship with the low wave steepness $kA = 0.0034$ are almost same with the linear results. The case of $kA = 0.034$ does not improve much compared to that at the smallest wave steepness; even the wave steepness is almost 10 times larger. For the case of $kA = 0.067$, it seems that the nonlinear effects associated with free surface conditions are more pronounced near the piston-mode frequency, which means after a certain wave steepness, the influence of wave nonlinearity becomes prominent very rapidly.

5. Conclusions

We reformulate the fully nonlinear potential wave model by subtracting a prescribed nonlinear incident wave and solve the scattered wave field only by a higher order boundary element time-domain simulation. Wave resonances in the gap between two side-by-side barges are captured. Comparisons with linear results and experiments suggest that nonlinear effects associated with free surface conditions may not be negligible when a steep wave is considered, in addition to the viscous effects.

References

[1] Molin, B., Remy, F., Kimmoun, O., Stassen, Y. 2002, Experimental Study of the Wave Propagation and Decay in a Channel through a Rigid Icesheet, *Applied Ocean Research*, No. 24, pp. 247–260.

[2] Newman, J.N. 2003, Application of Generalized Modes for the Simulation of Free Surface Patches in Multiple Body Interactions, *WAMIT Consortium Report*.

[3] Chen, X.B. 2004, Hydrodynamics in Offshore and Naval Applications Part 1, *Proc. of 6th Intl. Conf. on Hydrodynamics* (Perth).

[4] Pauw, W.H., Huijsmans, R.H.M., Voogt, A. 2007, Advances in the Hydrodynamics of Side-by-side Moored Vessels, *Proc. of 26th Intl. Conf. OMAE2007*, (San Diego).

[5] Kristiansen, T., Faltinsen, O.M. 2008, Application of a Vortex Tracking Method to the Piston-like Behavior in a Semi-entrained Vertical Gap, *Applied Ocean Research*, No. 30, pp. 1–16.

[6] Molin, B., Remy F., Camhi, A., Ledoux, A. 2009, Experimental and Numerical Study of the Gap Resonances in-between Two Rectangular Barges, *Proc. of 13th Cong. of International Maritime Association of Mediterranean IMAM*, (Istanbul).

[7] Bai, W., Eatock Taylor, R. 2006, Higher-order Boundary Element Simulation of Fully Nonlinear Wave Radiation by Oscillating Vertical Cylinder, *Applied Ocean Research*, No. 28, pp. 247–265.